Efficient Gridless Wideband Direction-of-Arrival Estimation From Many Frequencies

Yiming Zhou* Huayu Fu† Wei Dai*
*Department of Electrical and Electronic Engineering, Imperial College London, UK
†Xingjian College, Tsinghua University, China

***Abstract*—This paper addresses gridless direction-of-arrival (DOA) estimation for unknown source signals across a wide frequency range. While processing signals jointly across multiple frequencies can improve DOA estimation accuracy, it significantly increases computational complexity as the model size expands, rendering traditional methods impractical for handling many frequencies. To improve computational efficiency, we apply the Hankel matrix lifting technique, casting the DOA estimation as a nonconvex low-rank Hankel matrix recovery problem. A crucial aspect of our method is that the optimization matrix variable possesses both low-rank and Hankel structures, which allows for efficient computations of matrix-vector products, truncated singular value decomposition (SVD), and gradient and Newton direction evaluations. By leveraging a modern second-order nonconvex optimization technique, our approach achieves a low computational cost per iteration and a fast overall convergence rate. We quantify the per-iteration complexity of our method, and demonstrate its superiority compared with benchmark approaches. Numerical simulations confirm that our approach not only reduces computational complexity but also improves empirical DOA estimation accuracy.**

***Index Terms*—Gridless large-scale DOA estimation, low-rank Hankel matrix completion, nonconvex optimization.**

I. Introduction

Direction-of-arrival (DOA) estimation is a fundamental problem in array signal processing [1], with broad applications in radar [2], patient tracking [3], wireless communications [4], and much more. The task is to retrieve angles by estimating the (spatial) frequencies of several complex sinusoids from their superposition. Traditional DOA estimation methods for narrow-band signals, e.g., multiple signal classification (MUSIC) [5], and estimation of signal parameters via rotational invariant techniques (ESPRIT) [6], were among the first to be developed. However, these methods cannot be applied directly to wideband signals since the steering vectors are frequency dependent. To address this issue, a series of covariance matrix based methods are proposed, by leveraging nonlinear maps among covariance matrices across frequencies. This includes but not limited to signal subspace method (ISSM) [7], coherent signal subspace method (CSSM) [8], test of orthogonality of projected subspaces method (TOPS) [9], etc.

In recent years, significant efforts have been put on constructing a discrete grid of angles and applying sparse recovery techniques [10]–[12]. This approach reduces the need for extensive sampling across snapshots for covariance matrix estimation. However, its performance is heavily dependent on the granularity of the grid: ultra-fine grids can lead to high computational complexity and severe ill-posedness of the inverse problem, while coarse grids are plagued by unavoidable grid-mismatch issues.

More recently, methods targeting gridless wideband DOA estimation have emerged to address the grid mismatch issue. One approach involves convex relaxation of the problem by minimizing either the atomic norm or the nuclear norm. For instance, [13], [14] formulates the problem as atomic norm minimization (ANM) and derives the corresponding semidefinite programming (SDP) problem using Vandermonde decomposition [15]. Similarly, [16] converts the data into Hankel matrices and frames the DOA estimation as nuclear norm minimization. Although this method, known as EMaC, was not initially designed for wideband scenarios, it can be adapted for such applications. Both ANM and EMaC require full eigenvalue decomposition (EVD) or singular value decomposition (SVD) to solve the resulting convex problems. Specifically, the complexity of EVD for the non-structured matrix in ANM is $\mathcal{O}((MF+F)^3)$ [17], while the complexity of SVD for EMaC, when adapted in our formulation (8), is $\mathcal{O}(K^2MF^3)$. Here, K, M, and F represent the number of sources, sensors, and frequencies, respectively.

In this paper, we develop a computationally efficient and empirically effective method for wideband DOA estimation across multiple frequencies, building on our recent work [18]–[20]. We formulate the DOA estimation as a nonconvex low-rank Hankel matrix recovery problem. A key feature of this approach is that the optimization matrix variable exhibits both low-rank and Hankel structures, enabling efficient computation. To solve this nonconvex optimization problem, we adapt a recent Newton-type proximal algorithm, known as the Proximal Dogleg Opportunistic Majorization (PDOM) algorithm [21]. Tailored to the problem at hand, we construct a block-wise Hankel matrix with a carefully designed block size, which reduces the computational costs of all key steps—including matrix-vector products, truncated SVD of the structured matrix variable, and the gradient and Newton directions in the PDOM algorithm—by several orders of magnitude. Our analysis shows that the computational complexity per iteration is significantly reduced to $\mathcal{O}(KMF^2\log MF)$ compared to the aforementioned benchmarks. Numerical experiments demonstrate the fast convergence rate and substantial improvement in computational efficiency of the overall optimization procedure. Empirical results also indicate that our method achieves superior DOA estimation accuracy across a wide range of SNR levels, even with only a single snapshot of the data.

II. Problem Formulation

A. Signal Model

We consider a uniform linear array (ULA) with array spacing d of M sensors receiving wideband signals from K active sources located in the far field of the array. The knowledge on the model order is assumed to be known. Wideband signals from each source arrive from angles $\boldsymbol{\theta} = [\theta_1 \cdots \theta_K]^\top$, given in radians. Each signal has F temporal uniform frequency sub-bands, i.e., $f \in \{f_0, f_0+\Delta f, \ldots, f_0+(F-1)\Delta f\}$, where f_0 and Δf denotes the base frequency and frequency space, respectively. For notation simplicity, we denotes $\omega_k = \omega(\theta_k) := \frac{2\pi d\cos\theta_k}{c} \in \{-2\pi d/c, 2\pi d/c\}$. Based on above denotations, combing F frequency bins, the received signal can be formed as a matrix $\boldsymbol{Y} := [\boldsymbol{y}_1 \cdots \boldsymbol{y}_F] \in \mathbb{C}^{M\times F}$ with the following expression

$$\boldsymbol{Y} = \boldsymbol{X} + \boldsymbol{N}, \tag{1}$$

where

$$\boldsymbol{X} := \sum_{k=1}^{K} c_k \boldsymbol{A}(\omega_k) \otimes \boldsymbol{s}_k^\top$$
$$= \sum_{k=1}^{K} c_k [s_k(1)\boldsymbol{a}(f_0,\omega_k) \dots s_k(F)\boldsymbol{a}(f_0+(F-1)\Delta f,\omega_k)],$$

where c_k denotes the contribution of each source, $\boldsymbol{A}(\omega_k) := [\boldsymbol{a}(f_0,\omega_k)\cdots\boldsymbol{a}(f_0+(F-1)\Delta f,\omega_k)] \in \mathbb{C}^{M\times F}$, $\otimes$ is block Kronecker product, s_k records the signal amplitude for each frequency sub-band, $\boldsymbol{a}(f,w) := [1\dots e^{-j\omega f(M-1)}] \in \mathbb{C}^M$ is the steering vector corresponding to frequency f and DOA ω, and $\boldsymbol{N} \in \mathbb{C}^{M\times F}$ is Gaussian uncorrelated noise. The target is to obtain DOA information $\boldsymbol{\omega}$ from the observation $\boldsymbol{Y}$.

B. Optimization Problem

Inspired by line spectrum estimation via low-rank Hankel matrix recovery [22], [23], it can be shown that, for any signal $\boldsymbol{x} \in \mathbb{C}^M$ formed by a superposition of up to K narrow-band sources, its Hankel form admits a Vandermonde decomposition

$$\mathcal{H}\boldsymbol{x} = \boldsymbol{A}_N(\boldsymbol{\omega})\,\mathrm{diag}(\boldsymbol{s})\boldsymbol{A}_N^H(\boldsymbol{\omega}), \tag{2}$$

where $\mathcal{H}$ denotes a linear operator which maps $\boldsymbol{x}$ to a Hankel matrix $\mathcal{H}\boldsymbol{x} \in \mathbb{C}^{M_1\times M_2}$ with $M_1+M_2 = M+1$ as each element $[\mathcal{H}\boldsymbol{x}]_{i,j} = x_{i+j}, \forall i \in \{0,\dots,M_1-1\}, j \in \{0,\dots,M_2-1\}$ where index starts with zero, $\boldsymbol{A}_N(\boldsymbol{\omega}) = [\boldsymbol{a}(f_0,\omega_1)\cdots\boldsymbol{a}(f_0,\omega_K)] \in \mathbb{C}^{M_1\times K}$ is a Vandermonde matrix, $\boldsymbol{s} = [s_1\cdots s_K]^\top$. Since each element in a steering vector is unique and $K \le \min(M_1,M_2)$, $\boldsymbol{A}_N(\boldsymbol{\omega})$ is a full-rank matrix and $\mathrm{rank}(\mathcal{H}\boldsymbol{x}) \le K$. Therefore, given the observed signal $\boldsymbol{y}$, the problem can be formulated as

$$\min_{\boldsymbol{x}} \frac{1}{2}\|\boldsymbol{y}-\boldsymbol{x}\|_2^2 + \delta(\mathrm{rank}(\mathcal{H}\boldsymbol{x}) \le K), \tag{3}$$

where $\delta(\cdot)$ denotes the indicator function, which equals infinity if the condition is violated and zero otherwise.

The formulation (3) can be extended to the multi-channel line spectrum estimation [24]. For multiple measurement vectors (MMVs) case, given L snapshots, $\boldsymbol{X} \in \mathbb{C}^{M\times L}$, a block Hankel matrix is constructed by stacking the Hankel matrices formed from each snapshot horizontally, as follows

$$\mathcal{H}\boldsymbol{X} = [\mathcal{H}\boldsymbol{x}_1 \dots \mathcal{H}\boldsymbol{x}_L]. \tag{4}$$

Since each snapshot (channel) is modulated homogeneously, i.e., by the same sinusoid, the low-rank structure of the block Hankel matrix still holds. As a result, by using the same decomposition as (2), we have

$$\min_{\boldsymbol{X}} \frac{1}{2}\|\boldsymbol{Y}-\boldsymbol{X}\|_2^2 + \delta(\mathrm{rank}(\mathcal{H}\boldsymbol{X}) \le K). \tag{5}$$

However, for wideband signals, the low-rank constraint is violated due to varying temporal frequencies across different frequency bins, posing challenges in combining information from different channels. To ensure the low-rank Hankel model remains consistent with the wideband signal, we develop the extended manifold array vector to uniformly represent the heterogeneously modulating signals. That is

$$\boldsymbol{a}_{ext}(f_u,\omega) := [1\dots e^{-j\omega f_u(N-1)}] \in \mathbb{C}^N \tag{6}$$

$$\boldsymbol{A}_{ext}(\omega_k) := [\boldsymbol{a}(f_u,\omega_k)\dots\boldsymbol{a}(f_u,\omega_k)] \in \mathbb{C}^{N\times F}, \tag{7}$$

where $f_u = \mathrm{GCD}(f_0, f_0+\Delta f, \dots, f_0+(F-1)\Delta f)$ computes the greatest common divisor of all frequencies in the set of frequency bins, and $N = \frac{(f_0+(F-1)\Delta f)(M-1)}{f_u} + 1 \in \mathbb{Z}^+$. Therefore, the wideband DOA estimation via low-rank Hankel matrix completion can be formulated as

$$\min_{\boldsymbol{M},\boldsymbol{X}} F(\boldsymbol{M},\boldsymbol{X}) = \frac{1}{2}\|\boldsymbol{Y}-\mathcal{U}\boldsymbol{X}\|_F^2 + \frac{\alpha}{2}\|\boldsymbol{M}-\mathcal{H}\boldsymbol{X}\|_F^2 + \delta(\mathrm{rank}(\boldsymbol{M}) \le K), \tag{8}$$

where $\alpha > 0$, and $\boldsymbol{M} \in \mathbb{C}^{M_1\times M_2 F}$ is introduced for computational traceability. With low-rank assumption on $\boldsymbol{M}$, each block Hankel matrix is constructed as a tall matrix to allow efficient computations illustrated in Section III. Specifically, we set $M_2 = 3K$ and $M_1 = N-3K+1$ (on the order of MF). $\mathcal{U}: N\times F \to M\times F$ is a linear operator that maps the signal represented by the extended manifold array vector to the original domain. Specifically,

$$\boldsymbol{Y} = \mathcal{U}\boldsymbol{X} \to \boldsymbol{Y}(i,j) = \boldsymbol{X}(1+\frac{\Delta f}{f_u}(i-1)j, j). \tag{9}$$

III. Efficient Solver

The formulation in (8) is a nonconvex problem due to the rank constraint. A typical way to handle it is to consider the convex relaxation of low-rank constraint, i.e., the nuclear norm regularization [16]. However, optimizing the nuclear norm requires soft-thresholding on full scale SVD of M. The computational complexity for each iteration is on $\mathcal{O}(M_1M_2^2F^2) = \mathcal{O}(K^2MF^3)$, growing cubically with respect to the number of frequency bins, which becomes prohibitive for large-scale cases. Incidentally, the SDP of ANM requires $\mathcal{O}((MF+F)^3)$ per iteration, which also shares the same limitation.

To extend DOA estimation to many frequencies, we directly solve the nonconvex formulation (8) by adopting the proximal dogleg opportunistic majorization (PDOM) to enhance convergence speed in number of iterations [21]. The computational complexity per iteration is optimized by only solving K-truncated SVD and fully exploring the Hankel and low-rank structures in the update variable. In the remainder of this section, we first provide detailed implementation steps for applying PDOM to solve (8), followed by specific acceleration techniques for each computational operation.

To apply the PDOM, we first reformulate the multi-variable problem in (8) into a single-variable problem by expressing $\boldsymbol{X}$ as a function of $\boldsymbol{H}$. That is,

$$\nabla_{\boldsymbol{X}} F = \mathcal{U}^\star(\mathcal{U}(\boldsymbol{X})-\boldsymbol{Y}) + \alpha\mathcal{H}^\star(\mathcal{H}(\boldsymbol{X})-\boldsymbol{M}) = 0, \tag{10}$$

$$\boldsymbol{X}^\star = (\mathcal{U}^\star\mathcal{U} + \alpha\mathcal{H}^\star\mathcal{H})^{-1}(\mathcal{U}^\star\boldsymbol{Y} + \alpha\mathcal{H}^\star\boldsymbol{M}). \tag{11}$$

Here, $\mathcal{U}^\star$ and $\mathcal{H}^\star$ denote adjoint operators of $\mathcal{U}$ and $\mathcal{H}$, respectively. The operator $\mathcal{U}^\star\mathcal{U}$ represents a diagonal matrix whose kth diagonal elements is one if $k = 1+\frac{\Delta f}{f_u}(i-1)j + N(j-1)$ and zero otherwise. Similarly, $\mathcal{H}^\star\mathcal{H}$ is also a diagonal matrix with form of $\mathrm{diag}(\boldsymbol{h})$, where $\boldsymbol{h} = [1,\dots,M_1-1,\underbrace{M_1,\cdots,M_1}_{M_2-M_1+1},M_1-1,\dots,1]^\top$. For simplicity, we define $\boldsymbol{W} := (\mathcal{U}^\star\mathcal{U}+\alpha\mathcal{H}^\star\mathcal{H})^{-1}$, where $\boldsymbol{W}$ is the inverse of a diagonal matrix which can be computed with $\mathcal{O}(N)$ complexity. Substitute (11) to (8), we have

$$\min_{\boldsymbol{M}} \underbrace{\frac{1}{2}\|\boldsymbol{Y}-\mathcal{U}\boldsymbol{W}(\mathcal{U}^\star\boldsymbol{Y}+\alpha\mathcal{H}^\star\boldsymbol{M})\|_F^2 + \frac{\alpha}{2}\|\boldsymbol{M}-\mathcal{H}\boldsymbol{W}(\mathcal{U}^\star\boldsymbol{Y}+\alpha\mathcal{H}^\star\boldsymbol{M})\|_F^2}_{q(\boldsymbol{M})} + \underbrace{\delta(\mathrm{rank}(\boldsymbol{M}) = K)}_{h(\boldsymbol{M})}, \tag{12}$$

where $q(\boldsymbol{M})$ and $h(\boldsymbol{M})$ denote the smooth and nonsmooth terms. Then we construct the gradient, Newton directions, and surrogate function for the PDOM algorithm. The gradient can be computed by the trick in [25], we have

$$\begin{aligned}\boldsymbol{g} &= \nabla_{\boldsymbol{M}} F + \nabla_{\boldsymbol{X}^\star} F \nabla_{\boldsymbol{M}} \boldsymbol{X}^\star \\ &\overset{(a)}{=} \nabla_{\boldsymbol{M}} F + \boldsymbol{0} \\ &= \alpha(\boldsymbol{M} - \alpha\mathcal{H}\boldsymbol{W}\mathcal{H}^\star\boldsymbol{M} - \mathcal{H}\boldsymbol{W}\mathcal{U}^\star\boldsymbol{Y}),\end{aligned} \tag{13}$$

where (a) is due to the optimality condition (10). The Hessian matrix takes the form of

$$\boldsymbol{Q} = \alpha\boldsymbol{I} - \alpha^2\mathcal{H}\boldsymbol{W}\mathcal{H}^\star, \tag{14}$$

where $\boldsymbol{I}$ is an identity matrix. To compute the inverse of the Hessian matrix, we use Woodbury matrix identity $(\boldsymbol{I}+\boldsymbol{U}\boldsymbol{V})^{-1} = \boldsymbol{I}-\boldsymbol{U}(\boldsymbol{I}+\boldsymbol{V}\boldsymbol{U})^{-1}\boldsymbol{V}$ [26], one has

$$\begin{aligned}\boldsymbol{Q}^{-1} &= \frac{1}{\alpha}\left(\boldsymbol{I}-\alpha\mathcal{H}\boldsymbol{W}\mathcal{H}^{\star}\right)^{-1} \\ &= \frac{1}{\alpha}\left(\boldsymbol{I}-\mathcal{H}\left(\boldsymbol{I}-\alpha\boldsymbol{W}\mathcal{H}^{\star}\mathcal{H}\right)^{-1}\alpha\boldsymbol{W}\mathcal{H}^{\star}\right) \\ &= \frac{1}{\alpha}\left(\boldsymbol{I}-\alpha\mathcal{H}\tilde{\boldsymbol{D}}\boldsymbol{W}\mathcal{H}^{\star}\right), \end{aligned} \tag{15}$$

where $\tilde{\boldsymbol{D}} = (\boldsymbol{I}-\alpha\boldsymbol{W}\mathcal{H}^{\star}\mathcal{H})^{-1}$ is also the inverse of a diagonal matrix. Consequently, computing the Newton direction $\boldsymbol{g}_N = -\boldsymbol{Q}^{-1}\boldsymbol{g}$ avoids the need for dense matrix inversion. PDOM belongs to the majorization-minimization algorithms and the special surrogate function of $q(\boldsymbol{M})$ optimized for each iteration is defined as

$$\begin{aligned}m_{\beta}(\boldsymbol{M};\boldsymbol{M}^k) := q(\boldsymbol{M}^k) + \operatorname{Tr}\left(\boldsymbol{g}_{\beta}^{\top}\left(\boldsymbol{M}-\boldsymbol{M}^k\right)\right) \\ +\frac{1}{\tau_{\beta}}\left\|\boldsymbol{M}-\boldsymbol{M}^k\right\|_F^2, \end{aligned} \tag{16}$$

where k denotes the iteration index, and $\operatorname{Tr}(\cdot)$ computes the trace of a matrix. Here, for $\beta \in (0,1]$, we define

$$\boldsymbol{g}_{\beta} := \frac{\operatorname{Tr}\left(\boldsymbol{g}^{\top}\boldsymbol{p}(\beta)\right)}{\|\boldsymbol{p}(\beta)\|^2}\boldsymbol{p}(\beta), \quad \tau_{\beta} := -\frac{\|\boldsymbol{p}(\beta)\|^2}{\operatorname{Tr}\left(\boldsymbol{g}^{\top}\boldsymbol{p}(\beta)\right)},$$

where $\boldsymbol{p}(\beta) := (\beta-1)\tau\boldsymbol{g}+\beta\boldsymbol{g}_N$ denotes the descent direction of PDOM and $\tau \in (0, 1/L_q)$, where L_q is the Lipschitz constant of the gradient of the smooth part q. Finally, given β, the overall surrogate function $m_{\beta}(\boldsymbol{M};\boldsymbol{M}^k)+h(\boldsymbol{M})$ for each iteration can be solved by one proximal operator,

$$\boldsymbol{M}^{k+1} = \operatorname{prox}_{\tau_{\beta^k}h}\left(\boldsymbol{M}^k+\boldsymbol{p}(\beta^k)\right) = \operatorname{TSVD}\left(\boldsymbol{M}^k+\boldsymbol{p}(\beta^k)\right), \tag{17}$$

where $\operatorname{TSVD}(\cdot)$ computes the K-truncated SVD of the given matrix.

After completing the low-rank Hankel matrix by PDOM, the DOAs are extracted using a subspace-based method. Unlike the traditional MUSIC algorithm [27], which requires one step full-scale SVD to identify the noise-space correlation function, we utilize the results of truncated SVD from the final iteration and apply Gram-Schmidt Orthogonalization [28] on the left singular matrix $\boldsymbol{U} \in \mathbb{C}^{M_1\times K}$ to compute the noise subspace $\boldsymbol{U}_2 \in \mathbb{C}^{M_1\times K}$. Subsequently, we identify the DOAs by locating the K largest local maxima of the image function. The image function is defined as

$$J(\hat{\boldsymbol{\omega}}) = \frac{\left\|\phi^{M_1}(\hat{\boldsymbol{\omega}})\right\|_2}{\left\|U_2^H\phi^{M_1}(\hat{\boldsymbol{\omega}})\right\|_2}, \tag{18}$$

where

$$\phi^{M_1}(\hat{\boldsymbol{\omega}}) = \begin{bmatrix} 1 & 1 & \dots & 1 \\ e^{-2\pi i\omega_1} & e^{-2\pi i\omega_2} & \dots & e^{-2\pi i\omega_s} \\ \left(e^{-2\pi i\omega_1}\right)^2 & \left(e^{-2\pi i\omega_2}\right)^2 & \dots & \left(e^{-2\pi i\omega_s}\right)^2 \\ \vdots & \vdots & \vdots & \vdots \\ \left(e^{-2\pi i\omega_1}\right)^{M_1} & \left(e^{-2\pi i\omega_2}\right)^{M_1} & \dots & \left(e^{-2\pi i\omega_s}\right)^{M_1} \end{bmatrix},$$

and $\hat{\boldsymbol{\omega}} = [\omega_1,\omega_2,\dots,\omega_s]^{\top} \in \mathbb{C}^s$ denotes the sample frequency. The overall procedure for efficient wideband DOA estimation is summarized in Algorithm 1.

Algorithm 1 Efficient DOA Estimation via **N**onconvex **L**ow-rank **H**ankel Matrix **C**ompletion with PDOM (NLHC-PDOM).

Require: Array measurement $\boldsymbol{Y}$, Model order K, the maximum number of iterations $k_{\max}$.

1: Initialize: $\boldsymbol{M}^0 \in \mathbb{C}^{M_1\times M_2F}$, $\tau \in (0, 1/L_q)$, $k = 0$.
2: **while** the stopping criterion is not satisfied and $k < k_{\max}$ **do**
3: Compute $\boldsymbol{M}^{k+1}$ using (17), for the largest value $\beta^k \in \left\{\frac{1}{2}^i \mid i \in \mathbb{N}\right\}$ such that $m_{\alpha^k}(\boldsymbol{M}^{k+1};\boldsymbol{M}^k) \geq q(\boldsymbol{M}^{k+1})$.
4: $k \leftarrow k+1$.
5: **end while**
6: Record K-truncated SVD of $\boldsymbol{M}^k$: $\boldsymbol{U},\boldsymbol{\Sigma},\boldsymbol{V}^H = \operatorname{TSVD}(\boldsymbol{M}^k)$.
7: Conduct Gram-Schmidt orthogonalization on $\boldsymbol{U}$ to generate $\boldsymbol{U}_2 \in \mathbb{C}^{M_1\times K}$.
8: Compute the imaging function by (18).
9: **Output:** $\boldsymbol{\omega}(\boldsymbol{\theta}) = \{$the K largest local maxima of $J(\hat{\boldsymbol{\omega}})\}$.

A. Computational Complexity Analysis

One favorable feature of Algorithm 1 is its low computational complexity per iteration. In this section, we present the details of exploiting Hankel and low-rank structures to achieve that. The primary operations contributing to the computational complexity include the following.

(1) Hankel operator $\mathcal{H}\boldsymbol{X}$: In Algorithm 1, the Hankel matrix is consistently represented by the original matrix $\boldsymbol{X}$. As a result, no additional computational effort is needed to explicitly construct the Hankel matrix.

(2) Adjoint Hankel operator $\mathcal{H}^{\star}\boldsymbol{M}$: Since low-rank matrix $\boldsymbol{M} \in \mathbb{C}^{M_1\times M_2F}$ is stored by its truncated SVD $\boldsymbol{M} = \boldsymbol{U}\boldsymbol{\Sigma}\boldsymbol{V}^H$, for ith block Hankel matrix $\boldsymbol{M}_i \in \mathbb{C}^{M_1\times M_2}$ corresponding to $\mathcal{H}\boldsymbol{x}_i$, we have

$$\mathcal{H}^{\star}\boldsymbol{M}_i = \mathcal{H}^{\star}\boldsymbol{U}\boldsymbol{\Sigma}\boldsymbol{V}_i^H = \sum_{j=1}^{K}\Sigma_j\boldsymbol{U}[:,j] * \boldsymbol{V}_i^H[j,:], \tag{19}$$

where $\boldsymbol{V}_i^H = \boldsymbol{V}^H[:, 1+M_2(i-1) : M_2i]$, and $*$ denotes convolution, which can be computed efficiently by FFT with $\mathcal{O}(K(MF+K)\log(MF+K)) = \mathcal{O}(KMF\log MF)$. For the overall $\mathcal{H}^{\star}\boldsymbol{M}$, the complexity is $\mathcal{O}(KMF^2\log MF)$

(3) Hankel matrix multiplication with a vector: Assume that the Hankel matrix $\boldsymbol{H}$ is mapped from the original matrix $\boldsymbol{X}$, the fast multiplication is performed by 1-D FFT with complexity $\mathcal{O}(MF^2\log MF)$ [29].

(4) Low-rank matrix multiplication with a vector: Since the truncated SVD of $\boldsymbol{M}$ is known, the multiplication with a vector is performed as $\boldsymbol{M}\boldsymbol{x} = \boldsymbol{U}\boldsymbol{\Sigma}\boldsymbol{V}^H\boldsymbol{x}$ which requires $\mathcal{O}(KMF) + \mathcal{O}(K) + \mathcal{O}(K^2F) = \mathcal{O}(KMF+K^2F)$.

(5) K-trancated SVD: This operation dominates the complexity per iteration. For each iteration, the proximal operator is performed on a linear combination of a low-rank matrix $\boldsymbol{M}^k$ and a Hankel matrix $\boldsymbol{p}(\beta^k)$. With the knowledge of truncated SVD of $\boldsymbol{M}^k$ and fast Hankel matrix vector multiplication, the fast K-trancated SVD achieved by the Lanczos bidiagonalization [30] has the computational complexity of $\mathcal{O}(K^2MF+K^3F+KMF^2\log MF)$.

(6) Surrogate function for PDOM: Computing (16) requires matrix multiplication and summation of each element of a matrix which has the complexity of $\mathcal{O}(KMF^2)$.

For the other operations, such as computing (11), gradients, and Newton directions for PDOM, these can be efficiently executed using the aforementioned six steps and the inversion of the diagonal matrix. The overall computational complexity per iteration is $\mathcal{O}(KMF^2\log MF)$, given $F \gg M > K$.

IV. NUMERICAL EXPERIMENTS

In this section, we conduct numerical experiments to evaluate the performance of the proposed NLHC-PDOM method for wideband DOA estimation. The comparative analysis is performed with baseline methods ANM [13] and EMaC [16], and CRB [31]. We exclude [20] from comparison because the errors reported in the original literature are comparatively higher than those of our method. For

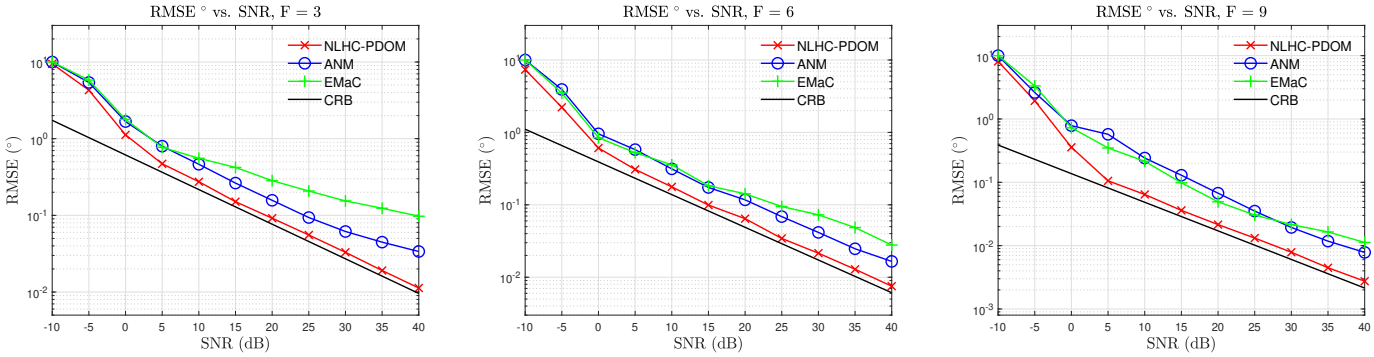

Fig. 2: RMSE in degress vs. SNR for $M = 10$, and $K = 3$ across three different frequency settings. The DOAs are randomly selected and vary for each trial.

the noisy cases, we follow the strategy in [32] to suppress noise for ANM model. The equivalent SDP is solved by well-established CVX toolbox. All experiments are executed using Julia on a Windows 11 laptop with an Intel i7-11800H CPU and 32 GB of RAM.

For each experiment and realization, K DOAs are randomly generated from a uniform distribution with range $[10°, 170°]$, with a minimum separation $\frac{4}{M}$, unless a specific angle set is chosen. The frequency amplitude vectors $\boldsymbol{s}_k$ are randomly generated with standard complex normal distribution $\mathcal{CN}(0, 1)$ and then normalized to have unit norm. The uniform frequency set is considered where $\Delta f = f_0$ and the array spacing of ULA is $d = \frac{c}{2Ff_0}$. The additive noise $\boldsymbol{N}$ is drawn from a a complex Gaussian distribution $\mathcal{CN}(0, \sigma^2)$ and the signal-to-noise ratio (SNR) is computed as $\text{SNR} = 20\log_{10}\frac{\|\boldsymbol{X}\|_F}{\|\boldsymbol{N}\|_F}$. Estimation accuracy is measured the root mean square error (RMSE) between the true DOAs, $\boldsymbol{\theta}_k$, and the recovered DOAs, $\hat{\boldsymbol{\theta}}_k$, that is $\text{RMSE} = \sqrt{\mathbb{E}\left[\frac{1}{K}\sum_{k=1}^{K}\left(\boldsymbol{\theta}_k - \hat{\boldsymbol{\theta}}_k\right)^2\right]}$. To ensure that the resolution of the MUSIC algorithm does not introduce any bias in the estimation accuracy, we set $\hat{\boldsymbol{\omega}} \in \mathbb{C}^{64000}$. The tested algorithms are terminated if $\left\|\boldsymbol{M}^k - \boldsymbol{M}^{k-1}\right\|_F^2 < 10^{-4}$ or $k > 10^4$. $\alpha = 1$.

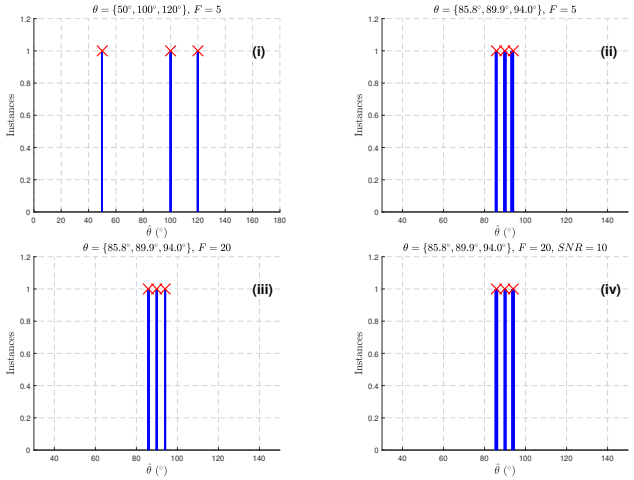

Fig. 1: Histogram of the estimated DOAs by NLHC-PDOM (the blue vertical lines) for 10 trials. True DOAs are indicated by ×. $M = 5$. For each trial, the initial point $\boldsymbol{M}^0$ (randomly selected) and the frequency amplitude $\boldsymbol{s}_k$ are different.

We first evaluate the proposed method across four scenarios, varying the separation conditions of DOAs, the number of frequencies, and the SNR. Results are detailed in Fig. 1. The NLHC-PDOM

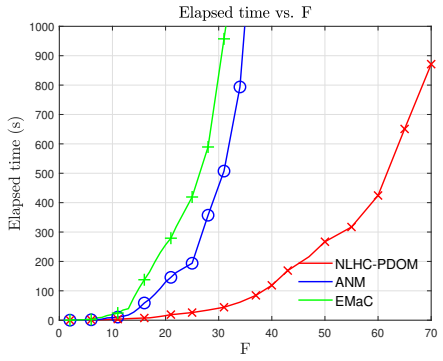

Fig. 3: Average runtime (s) vs. F for $M = 5$, $K = 2$, 5 trials, and noise-free.

algorithm consistently avoids misidentifying DOAs with obvious errors. Sub-figures (ii) and (iii) illustrate the benefits of incorporating additional frequencies, as the estimated DOAs are more tightly concentrated around the true values.

Fig. 2 presents the performance of each algorithm at different SNR levels, along with the CRB. Each point in the figure represents the average results from 50 independent trials. While increasing the number of trials is desirable, it is important to note that ANM and EMaC become significantly slower as the number of frequencies increases. The NLHC-PDOM method outperforms other gridless techniques in terms of a smaller gap to the CRB in three cases.

To highlight the computational efficiency, we compare the operation time of each algorithm for different values of F. The results, shown in Fig. 3, are truncated when the time exceeds 1000 seconds. The proposed method reduces the running time for several orders of magnitude. Detailed results on the fast convergence rate in terms of iterations will be provided in the extended journal version, though Fig. 3 already reflects the fast convergence in overall runtime.

V. CONCLUSION

This paper develops a computationally efficient gridless DOA estimation method for many frequencies. The problem is formulated as a nonconvex low-rank Hankel matrix completion and solved by a second-order proximal algorithm to achieve fast convergence. With the help of low-rank and Hankel structures, the computational complexity is significantly reduced by accelerated truncated SVD and fast matrix vector multiplication. Numerical results demonstrate both the high computational efficiency and the improved accuracy of our method, as evidenced by much less operation time and a smaller gap to the CRB.

REFERENCES

[1] H. Krim and M. Viberg, "Two decades of array signal processing research: The parametric approach," *IEEE signal processing magazine*, vol. 13, no. 4, pp. 67–94, 1996.

[2] A. Hassanien and S. A. Vorobyov, "Transmit energy focusing for doa estimation in mimo radar with colocated antennas," *IEEE Transactions on Signal Processing*, vol. 59, no. 6, pp. 2669–2682, 2011.

[3] L. Wan, G. Han, L. Shu, S. Chan, and T. Zhu, "The application of doa estimation approach in patient tracking systems with high patient density," *IEEE Transactions on Industrial Informatics*, vol. 12, no. 6, pp. 2353–2364, 2016.

[4] C. Vasanelli, F. Roos, A. Durr, *et al.*, "Calibration and direction-of-arrival estimation of millimeter-wave radars: A practical introduction," *IEEE Antennas and Propagation Magazine*, vol. 62, no. 6, pp. 34–45, 2020.

[5] R. Schmidt, "Multiple emitter location and signal parameter estimation," *IEEE transactions on antennas and propagation*, vol. 34, no. 3, pp. 276–280, 1986.

[6] R. Roy and T. Kailath, "Esprit-estimation of signal parameters via rotational invariance techniques," *IEEE Transactions on acoustics, speech, and signal processing*, vol. 37, no. 7, pp. 984–995, 1989.

[7] M. Wax, T.-J. Shan, and T. Kailath, "Spatio-temporal spectral analysis by eigenstructure methods," *IEEE transactions on acoustics, speech, and signal processing*, vol. 32, no. 4, pp. 817–827, 1984.

[8] H. Wang and M. Kaveh, "Coherent signal-subspace processing for the detection and estimation of angles of arrival of multiple wide-band sources," *IEEE Transactions on Acoustics, Speech, and Signal Processing*, vol. 33, no. 4, pp. 823–831, 1985.

[9] Y.-S. Yoon, L. M. Kaplan, and J. H. McClellan, "Tops: New doa estimator for wideband signals," *IEEE Transactions on Signal processing*, vol. 54, no. 6, pp. 1977–1989, 2006.

[10] L. Wang, L. Zhao, G. Bi, C. Wan, L. Zhang, and H. Zhang, "Novel wideband doa estimation based on sparse bayesian learning with dirichlet process priors," *IEEE Transactions on Signal Processing*, vol. 64, no. 2, pp. 275–289, 2015.

[11] C. Liu, Y. V. Zakharov, and T. Chen, "Broadband underwater localization of multiple sources using basis pursuit de-noising," *IEEE Transactions on Signal Processing*, vol. 60, no. 4, pp. 1708–1717, 2011.

[12] J.-A. Luo, X.-P. Zhang, and Z. Wang, "A new subband information fusion method for wideband doa estimation using sparse signal representation," in *2013 IEEE International Conference on Acoustics, Speech and Signal Processing*, IEEE, 2013, pp. 4016–4020.

[13] Y. Wu, M. B. Wakin, and P. Gerstoft, "Gridless doa estimation with multiple frequencies," *IEEE transactions on signal processing*, vol. 71, pp. 417–432, 2023.

[14] Y. Wu, M. B. Wakin, and P. Gerstoft, "Non-uniform array and frequency spacing for regularization-free gridless doa," *IEEE Transactions on Signal Processing*, 2024.

[15] G. Tang, B. N. Bhaskar, P. Shah, and B. Recht, "Compressed sensing off the grid," *IEEE transactions on information theory*, vol. 59, no. 11, pp. 7465–7490, 2013.

[16] Y. Chen and Y. Chi, "Robust spectral compressed sensing via structured matrix completion," *IEEE Transactions on Information Theory*, vol. 60, no. 10, pp. 6576–6601, 2014.

[17] H. Jiang, T. Kathuria, Y. T. Lee, S. Padmanabhan, and Z. Song, "A faster interior point method for semidefinite programming," in *2020 IEEE 61st annual symposium on foundations of computer science (FOCS)*, IEEE, 2020, pp. 910–918.

[18] X. Yao and W. Dai, "A projected proximal gradient method for efficient recovery of spectrally sparse signals," in *2023 31st European Signal Processing Conference (EUSIPCO)*, IEEE, 2023, pp. 1738–1742.

[19] X. Yao and W. Dai, "Accelerated recovery of spectrally sparse signals viamodified proximal gradient in hankel space," in *ICASSP 2024-2024 IEEE International Conference on Acoustics, Speech and Signal Processing (ICASSP)*, IEEE, 2024, pp. 9476–9480.

[20] Z. Guo and W. Dai, "Gridless joint multi-band doa estimation for spectrum sensing," in *2023 IEEE 9th International Workshop on Computational Advances in Multi-Sensor Adaptive Processing (CAMSAP)*, IEEE, 2023, pp. 311–315.

[21] Y. Zhou and W. Dai, "Proximal dogleg opportunistic majorization for nonconvex and nonsmooth optimization," *arXiv preprint arXiv:2402.19176*, 2024.

[22] X. Zhang, Y. Liu, and W. Cui, "Spectrally sparse signal recovery via hankel matrix completion with prior information," *IEEE Transactions on Signal Processing*, vol. 69, pp. 2174–2187, 2021.

[23] X. Wu, Z. Yang, P. Stoica, and Z. Xu, "Maximum likelihood line spectral estimation in the signal domain: A rank-constrained structured matrix recovery approach," *IEEE Transactions on Signal Processing*, vol. 70, pp. 4156–4169, 2022.

[24] Y. Li and Y. Chi, "Off-the-grid line spectrum denoising and estimation with multiple measurement vectors," *IEEE Transactions on Signal Processing*, vol. 64, no. 5, pp. 1257–1269, 2015.

[25] X. Yao and W. Dai, "A low-rank projected proximal gradient method for spectral compressed sensing," *arXiv preprint arXiv:2405.07739*, 2024.

[26] M. A. Woodbury, *Inverting modified matrices*. Department of Statistics, Princeton University, 1950.

[27] W. Liao and A. Fannjiang, "Music for single-snapshot spectral estimation: Stability and super-resolution," *Applied and Computational Harmonic Analysis*, vol. 40, no. 1, pp. 33–67, 2016.

[28] Å. Björck, "Numerics of gram-schmidt orthogonalization," *Linear Algebra and Its Applications*, vol. 197, pp. 297–316, 1994.

[29] L. Lu, W. Xu, and S. Qiao, "A fast svd for multilevel block hankel matrices with minimal memory storage," *Numerical Algorithms*, vol. 69, no. 4, pp. 875–891, 2015.

[30] K. Browne, S. Qiao, and Y. Wei, "A lanczos bidiagonalization algorithm for hankel matrices," *Linear algebra and its applications*, vol. 430, no. 5-6, pp. 1531–1543, 2009.

[31] Y. Liang, W. Liu, Q. Shen, W. Cui, and S. Wu, "A review of closed-form cramér-rao bounds for doa estimation in the presence of gaussian noise under a unified framework," *Ieee Access*, vol. 8, pp. 175 101–175 124, 2020.

[32] Y. Chi, "Guaranteed blind sparse spikes deconvolution via lifting and convex optimization," *IEEE Journal of Selected Topics in Signal Processing*, vol. 10, no. 4, pp. 782–794, 2016.